

Simulation of the Longitudinal Instability in ATF Damping Ring

Eun-San Kim, KEK, 1-1 Oho, Tsukuba-shi, Ibaraki-ken, 305, Japan

Abstract

A simulation was performed to study single bunch instability in ATF damping ring. We investigate the single bunch behavior of the ATF damping ring using time domain multiparticle tracking and a Vlasov equation approach.

1 INTRODUCTION

The beam current is often limited by coherent instabilities. These instabilities can occur either in the longitudinal or in the transverse directions. Longitudinal ones which we consider here often cause bunch lengthening or an increase of the loss rate. Bunch lengthening behavior has been observed in the ATF damping ring. Its measurement was performed below 5.5×10^9 in the bunch population. It is also interesting to predict the threshold for instability by a simulation method to operate the ATF damping ring below threshold.

The simulations were begun with the purpose to understand instability in the ATF damping ring. Below the threshold we have merely a bunch lengthening due to the potential well distortion. The average bunch shape due to potential well distortion has been performed for the ATF damping ring to obtain as function of currents[1]. Above the threshold we have also an increase of the energy spread within the bunch. Because the potential well distortion does not explain the energy spread growth, it is interesting to investigate the energy spread by tracking method. We found threshold for instability using multiparticle tracking. We describe the results of the simulation and then give a qualitative discussion on the instability in the ATF damping ring.

2 THE WAKEFIELD

We have attempted to find an approximate Green function wakefield $W(z)$ for the ATF damping ring using code MAFIA, MASK30 and ABCI, taking as driving bunch a short, Gaussian bunch with rms length of 1mm. To make it causal, the part on front of bunch center ($z < 0$) was reflected and added to the back (see Fig.1), a transformation that preserves the real part of the impedance.

To calculate V_{ind} we have used the same method used by Bane[2], i.e. binning the macroparticles in z without smoothing. The induced voltage on any turn is given by

$$V_{ind}(z) = -eN \int_{-\infty}^z W(z-z') \lambda_z(z') dz', \quad (1)$$

with N the bunch population and $\lambda_z(z)$ the longitudinal charge distribution. $W(z-z')$ is the Green function wake field.

3 MACROPARTICLE MOTION

To describe the electron's motion in a damping ring we use a standard multiparticle tracking method. The initial distributions of N_p macroparticles in the phase space are given with the potential well distribution. Each macroparticle i are tracked in phase space of position and energy coordinates (z_i, ϵ_i) with equations of motion which include radiation damping, radiation excitation and wakefield. The wakefield gives the effect on a macroparticle i from all macroparticles which precede it in the bunch and is a function of the phase space coordinates of macroparticle i as well as the macroparticles which precede it.

For tracking we let the beam be represented by N_p macroparticles; each particle i has position and energy coordinates (z_i, ϵ_i) . The longitudinal motion of the particle i is advanced on each turn according to the equations[2][3][4][5]:

$$\Delta \epsilon_i = -\frac{2T_o}{\tau_d} \epsilon_i + 2\sigma_{\epsilon o} \sqrt{\frac{T_o}{\tau_d}} r_i + V'_{rf} z_i + V_{ind}(z_i) \quad (2)$$

$$\Delta z_i = \frac{\alpha c T_o}{E_o} (\epsilon_i + \Delta \epsilon_i), \quad (3)$$

with T_o the revolution period, τ_d the damping time, $\sigma_{\epsilon o}$ the nominal rms energy spread, V'_{rf} the slope of the rf voltage (a negative quantity), α the momentum compaction factor, and E_o the nominal energy; r_i is a random number from a normal set with mean 0 and rms 1. The quantity V_{rf} is given by

$$V'_{rf} = w_{rf} \hat{V} [1 - (U_o/\hat{V})^2]^{1/2}, \quad (4)$$

where w_{rf} is the rf frequency, \hat{V} peak energy gain from rf and U_o average synchrotron radiation energy loss per turn.

For the simulations we take $T_o = 460$ ns, $E_o = 1.3$ GeV, rf frequency $\nu_{rf} = 714$ MHz, $\sigma_{\epsilon o} = 5.46775 \times 10^{-4}$, and $\tau_d = 20$ ms. Therefore $\nu_{so} T_o = 242$ turns, $\tau_d/T_o = 43272$ turns. We choose $V_{rf} = 0.2$ MV, where $\sigma_{zo} = 6.8$ mm, and the synchrotron frequency $\nu_{so} = 8.95$ kHz. We track the macroparticles for 3 longitudinal damping times.

In the simulations the statistical fluctuation in the beam distribution associated with the finiteness of the numbers of macroparticles can become rather large. The sensitivity of the results to the number of macroparticles was investigated. It was shown that the bunch length and energy spread were dependent on the number of macroparticles which were used in simulation. When we examine the dependence of the simulation results on the number of macroparticles, it is shown that there is no great differences

in the results if we track around 30000 macroparticles. To calculate λ_z in each turn we use 680 bins extending over $5\sigma_z$.

As a second method of calculation we use a computer program that solves perturbatively the time independent, linearized Vlasov equation, including the effects of potential well distortion, looking for unstable modes.

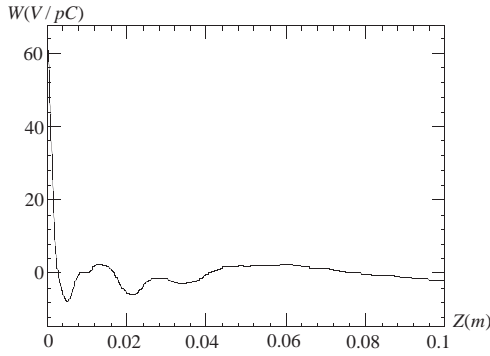


Figure 1: The wake field used for the simulation.

4 RESULTS

4.1 Average Bunch Distributions

On each turn we calculate the lower moments of the distributions. The average properties of the distributions are obtained by averaging over the last damping time. Figure 2 displays the average values of the σ_z , σ_ϵ and $\langle z \rangle$ as functions of current and also shows the Vlasov equation solution of σ_z . The tracking result shows lower bunch lengthening than Vlasov method. It is shown that the bunch shapes are more shifted forward than Gaussian due to the inductive ring. We see that the bunch lengthening in the damping ring is caused by both potential well distortion and energy spread due to inductive ring.

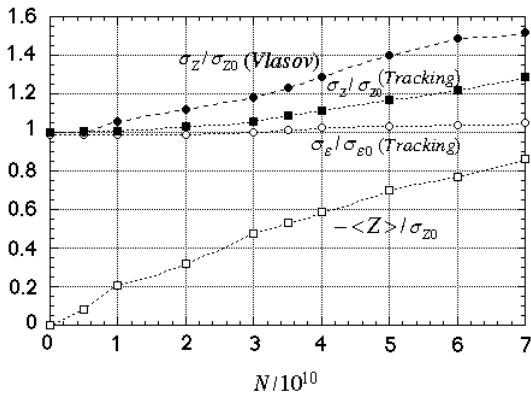


Figure 2: Average bunch properties vs number of particles in a bunch(N). Tracking results and the Vlasov method are shown.

Figure 3 shows bunch length oscillations for turns 129000-129816. Below threshold the moments of the distributions are well behaved and the period is seen to be around 130 turns, or about one-half the zero current synchrotron oscillation period. Above the threshold the oscillations undergo more perturbed macroscopic oscillations.

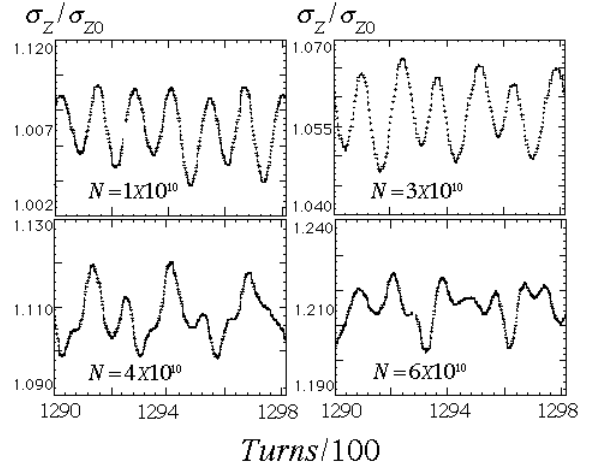


Figure 3: Bunch length oscillations for turns 129000-129816 for several current values. They show different types of bunch length oscillations before and after threshold ($N_{th} = 3.3 \times 10^{10}$).

4.2 The Threshold Current

The instability threshold is normally easy to find from the turn-by-turn tracking results. In Figure 2 the average rms energy spread as function of current is plotted. The result of the tracking shows very small energy spread compared to Vlasov method[1] and threshold $N_{th} = 3.3 \times 10^{10}$. A confirmation that this is the threshold current is the fact that the unstable mode in Vlasov method first appears at this current.

We note that the bunch lengthening is more increased due to the increase in energy spread above threshold. Above threshold the oscillations in the moments of the distribution obtained by tracking can be large and the pattern can vary greatly(see Figure 4).

4.3 Vlasov Equation Calculation

K.Oide and K.Yokoya have developed a theory to solve the time independent, linearized Vlasov equation including the effects of potential well distortion[6]. Using the wakefield of Figure 1 we take 6 azimuthal space harmonics and 60 mesh points in amplitude to represent phase space. We find that, due to the potential well distortion, the large gaps in mode frequencies have disappeared. It shows that the ATF damping ring is inductive.

The mode frequencies as function of N , as obtained by the Vlasov method are shown in Figure 5. A dot represents a stable mode, an 'X' an unstable mode, with its size proportional to the growth rate. The first and the strongest unsta-

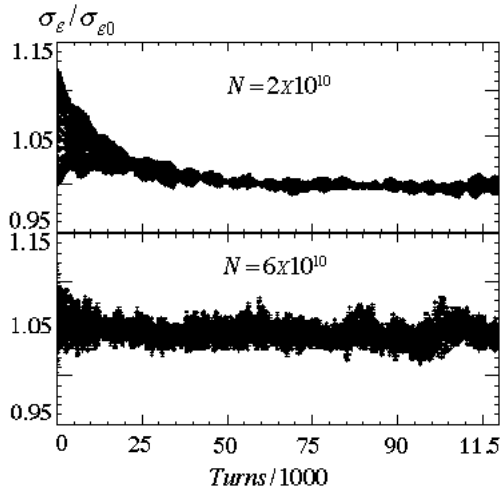


Figure 4: The turn-by-turn rms energy spread vs turn number.

ble mode is found at 3.3×10^{10} with a frequency of $2.9\nu_{s0}$. These facts were shown that the threshold for instability begins at 3.3×10^{10} when we find unstable state in more smaller interval N. The instability can be described as the coupling of two radial modes with the same azimuthal mode number.

Figure 6 gives contours of phase space of the unstable mode at $N=3.5 \times 10^{10}$ as calculated by the Vlasov equation. We see a sextupole mode that has been shifted forward.

4.4 Comparison with Measurement

The calculated bunch lengthening is much lower than the measurement which was performed by 5.5×10^9 . Bunch lengthening and threshold instability are expected to be estimated by measurements with more higher current.

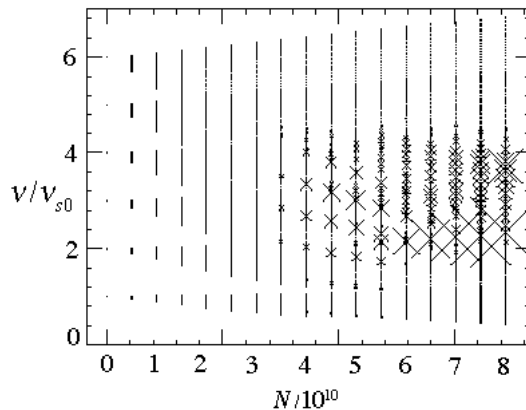


Figure 5: Modes obtained by the Vlasov method.

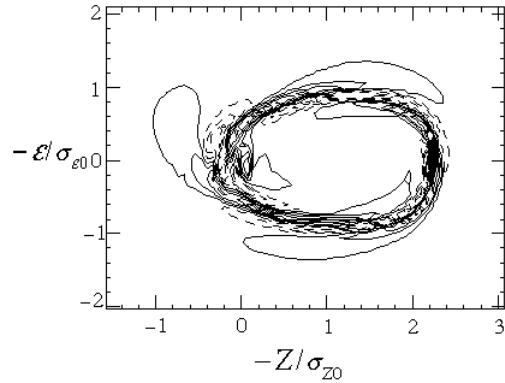


Figure 6: A contour plot of the unstable mode, obtained by solving the Vlasov equation, when $N = 3.5 \times 10^{10}$

5 ACKNOWLEDGMENTS

The author is grateful to Prof. K.Oide and Prof. Karl L. F. Bane for their helpful discussions. He has also greatly profited to the members of the ATF members.

6 REFERENCES

- [1] Eun-San Kim, this proceeding
- [2] K. Bane and K.Oide, Proc. of the 1993 IEEE Particle Acc. Conf., Washington D.C., 1993, p.3339.
- [3] K. Bane and K.Oide, Proc. of the 1993 IEEE Particle Acc. Conf., Washington D.C., 1993, p.3339.
- [4] R.Baartman and M.D'yachkov, Proc. of the 1996 IEEE Particle Acc. Conf., 1996, p.3119.
- [5] R.H. Siemann, Nucl. Instr. and Meth. 221 (1984) 294
- [6] K.Oide and K.Yokoya, KEK-Preprint-90-10, 1990.